

Chapter 5

Photonic Crystal H1-Defect Nanocavities: Towards Highly-Efficient Surface-Emitting Light Sources

5.1 Introduction

In previous chapter, the design of the very high Q -factor photonic crystal nanocavities has already been presented. However, when the situation comes to the realization of highly-efficient surface emitting light sources, only high Q -factor with small mode volume is insufficient to consider such light sources. The total efficiency of the light sources must be taken into account. The total efficiency can be shown as:

$$\text{Total efficiency } \eta_{\text{total}} = (\eta_{\text{coupling}}) \cdot (\eta_{\text{extract}}) \cdot (\eta_{\text{collection}}) \quad (5.1)$$

where η_{coupling} is the coupling efficiency, η_{extract} is the extraction efficiency, and $\eta_{\text{collection}}$ is the collection efficiency. η_{coupling} is defined as a fraction of the spontaneous emission (SE) that goes into the cavity mode and is determined by the Purcell factor as shown in the following expression :

$$\eta_{\text{coupling}} = \frac{F_p}{F_p + \frac{\gamma_l}{\gamma_0} + \frac{\gamma_{nr}}{\gamma_0}} \quad (5.2)$$

where F_p is the Purcell factor, γ_l is the spontaneous emission rate into noncavity modes, γ_{nr} is nonradiative recombination rate, and γ_0 is the spontaneous emission rate in free space. γ_l is usually approximated to be about γ_0 . η_{extract} is a fraction of the photons that are radiated out from the cavity into the vertical direction above the slab and can be defined as:

$$\eta_{\text{extract}} = \frac{\kappa_{d,\perp}}{\kappa_{d,\perp} + \kappa_{d,\parallel} + \kappa_e} \quad (5.3)$$

where $\kappa_{d,\perp}$ is the cavity decay rate in the vertical direction, $\kappa_{d,\parallel}$ is the cavity decay rate in the in-plane direction, and κ_e is the cavity decay rate due to imperfect crystal originated from fabrication process, e.g., scattering loss, absorption loss, etc. The cavity decay rate is inversely proportional to the Q -factor in the corresponding direction. Finally, $\eta_{\text{collection}}$ is a fraction of the photons that can be collected by an

objective lens or an optical fiber with the value of numerical aperture (NA) and can be calculated by:

$$\eta_{\text{collection}} = \frac{P_{\text{NA}}}{P_{\perp}} \quad (5.4)$$

where P_{NA} is the power vertically radiated into top side of the slab that can be collected by an optical fiber with NA, P_{\perp} is the all the power vertically radiated into top side of the slab.

From the last chapter, it has been already shown that the dipole mode of the designed cavity has a very large Purcell factor, in which the coupling efficiency very closed to 100% can be achieved. This means that almost all the spontaneously emitted photons are channel into a single mode (a cavity mode). In this chapter, the capability of the dipole mode of the H1-defect nanocavity to have both high extraction efficiency and collection efficiency will be discussed. In the last section, the total efficiency of the dipole mode of the H1-defect nanocavity will be discussed and shown to have high value compared to other structures reported so far.

5.2 Extraction Efficiency of Dipole Mode of H1-Defect Nanocavity

So far, there have been many reports on the extraction efficiency of the photonic crystal cavities. Some of them exploited micropillar structures based on a one-dimensional photonic crystal and achieved an extraction efficiency of about 40% [15], [30]. However, the micropillar structures can achieve much low Q -factor and large mode volume compared to those of two-dimensional photonic crystal nanocavities and also their efficiency violently suffers from the nonradiative recombination. There have also been reports on the extraction of photons based on a two-dimensional photonic crystal nanocavity by exploiting the evanescent coupling between a photonic crystal cavity and a tapered optical fiber [31], [32]. In those reports, photon collection efficiency of about 70% into a fiber was achieved. However, the Q -factor of the cavity significantly degraded due to the perturbation of the additional fiber.

To date, concept of designs for ultra-high Q -factor two-dimensional photonic crystal slab nanocavities has been concentrated on the elimination of the momentum components lying within the light line [7]-[11]. From Eq. (2.14), the expression of dispersion relation for a dielectric slab cladded by air is shown as:

$$\left(\frac{\omega}{c}\right)^2 = k_z^2 + k_\perp^2 \quad (5.1)$$

From this relation, the in-plane momentum components k_\perp that lie within the light line will lead to real value of the vertical momentum components k_z , which result in the vertical radiation losses. Hence the Q -factor of the cavity is limited. Anyway, removing the momentum components inside the light line also means difficulty to extract light out of the cavity toward the vertical direction. As a result, in those structures, there is a trade-off between Q -factor and extraction efficiency. However, the situation becomes different when it turns to be the case of H1-defect cavity. As discussed in previous chapter, the methodology of obtaining high Q -factor is not associated with the elimination of the momentum components lying within the light line. Therefore, it is possible to achieve both high Q -factor and high extraction efficiency in the same structure.

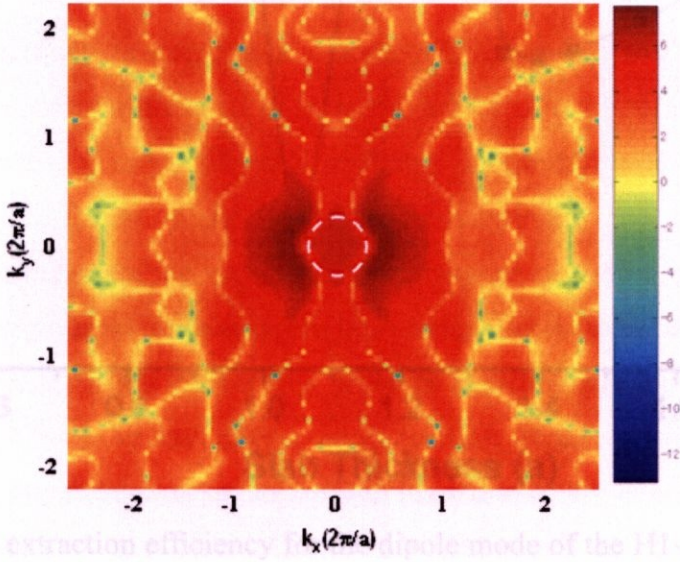


Figure 5.1 Field distribution of E_y component in momentum space shown in logarithm scale for the dipole mode of the H1-defect structure. Dashed line represents air light line. The region inside the dashed line is leaky region.

Figure 5.1 shows field distribution of the E_y component in momentum space shown in logarithm scale for the dipole mode of the H1-defect cavity with $r = 0.40a$ and $d = 1.35a$, which is the highest- Q structure from the previous chapter. This field distribution is the two-dimensional Fourier transform of the field distribution in real

space at the center of the slab. Dotted line shown in the figure represents air light line corresponding to normalized frequency of the defect mode. As observed in Fig. 5.1, the Fourier component of the dipole mode of the H1-defect cavity contains large elements inside the leaky region. As a result, the dipole mode of the H1-defect nanocavity has an ability to be efficiently extracted out of the cavity, that is, high extraction efficiency.

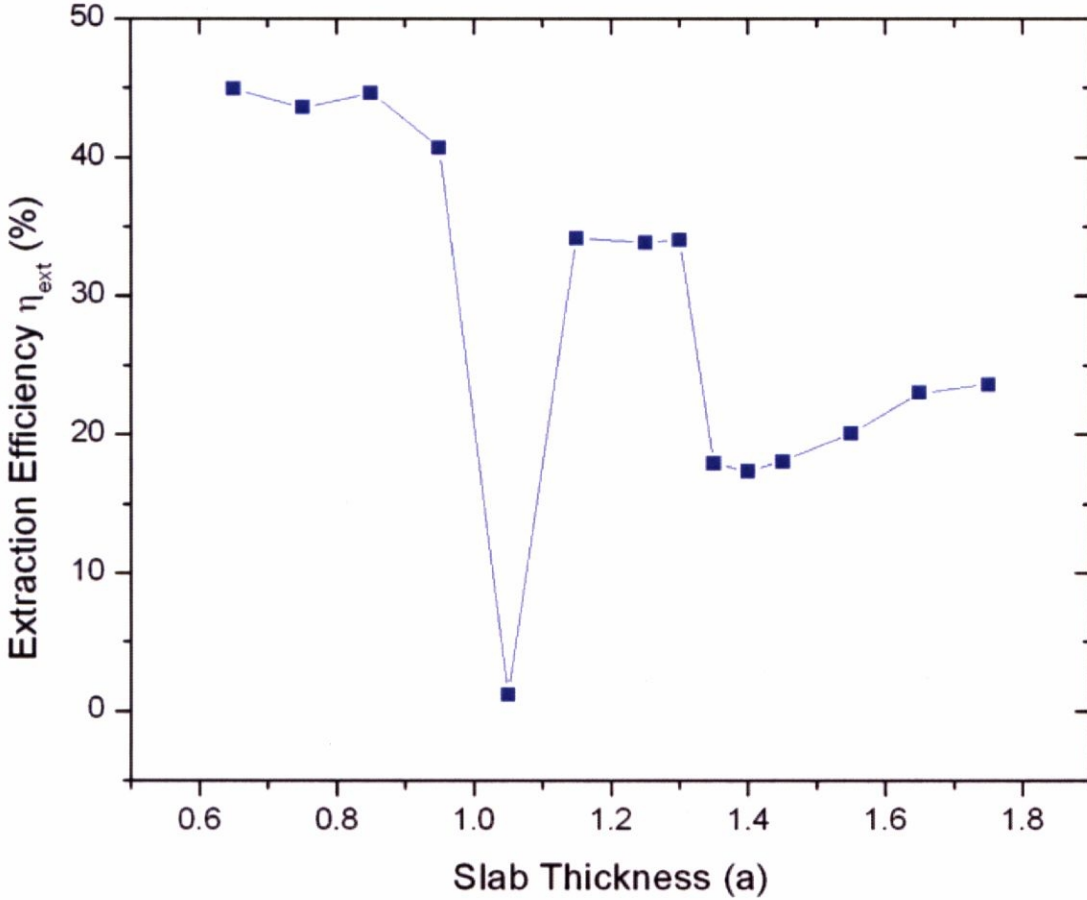


Figure 5.2 The extraction efficiency for the dipole mode of the H1-defect structure with $r = 0.40a$ that radiated out from the cavity toward vertical top-direction above the slab.

The extraction efficiency for the dipole mode of the H1-defect nanocavity is shown in Fig. 5.2 for the structure with $r = 0.40a$. The calculation of this plot excludes the effect of imperfect crystal originated from fabrication process ($\kappa_e = 0$). It should be noted that because the designed structure is an air-bridge slab, the ideal extraction efficiency is limited to only 50% due to its symmetry along the horizontal axis. Therefore, amounts of light vertically radiated out of the cavity into upper

direction and lower direction are identical. In the thin slab region, the extraction efficiency is more than 40% due to the large difference between the in-plane Q -factor and the vertical Q -factor. The minimum peak at the slab thickness around $1.00a$ is due to the coupling of the defect mode to the slab guided mode, in which light is guided through the slab and is hardly extracted out of the slab, so the extraction efficiency becomes near zero. In the thick slab region, it can be seen that the highest Q structure at the slab thickness of $1.35a$ has the extraction efficiency of only about 15%. This is because, as can be seen in Fig. 4.4(c), the vertical Q -factor is about two times higher than the in-plane Q -factor, therefore the extraction efficiency is limited.

5.3 Radiation Pattern of Dipole Mode of H1-Defect Nanocavity

As mentioned in the introduction section, the radiation pattern of the output light is another important factor needed to be considered in order to achieve highly-efficient surface emitting light sources, because it determines the collection efficiency. More concretely, the radiation pattern with Gaussian-like distribution is desirable because it can be simply and efficiently coupled to optical fibers. Although the Gaussian-like radiation pattern can be easily achieved in micropillar microcavities [14], [15], however, Q -factor of such structures is limited to low values due to transverse radiation losses along the pillar cross-section. The Q -factor of such structures can be enhanced by increasing the diameter of the pillar, but doing this yields larger mode volume. Therefore, the ratio of (Q/V_{eff}) is small. When the situation turns to the photonic crystal nanocavity, problem based on radiation pattern of light output emerges. That is to say, only a small fraction of the output photons can be collected by an objective lens or an optical fiber due to its complicated radiation pattern. An example of such a complicated radiation pattern can be seen else where [34]. As a result, a design of nanocavity as well as its cavity mode, which can achieve a Gaussian-like radiation pattern, is required in order to realize highly-efficient surface emitting light sources.

The radiation patterns of the output light are simulated by the FDTD method, by calculating the time averaged Poynting vector in the vertical direction at the plane positioned at $\sim 1\lambda$ above the surface of the slab. It should be noted that this position is corresponding to the far-field region. The radiation pattern of the dipole mode of the H1-defect cavity with $r = 0.40a$ and $d = 1.35a$ is calculated and shown in Fig. 5.3(a).

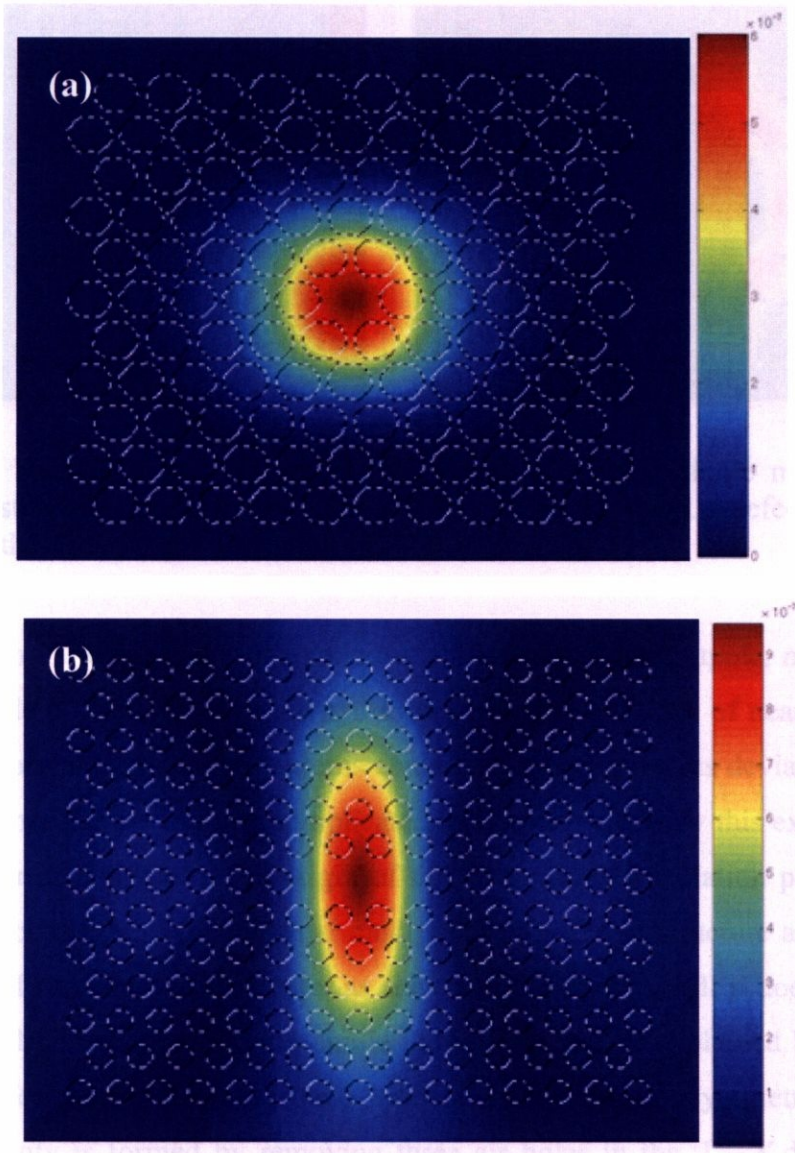


Figure 5.3 Radiation pattern of (a) the dipole mode of the H1-defect structure, and (b) the fundamental mode of the L3-defect structure, detected at about a wavelength above the slab. The Dotted circles show the size of the structure for reference.

The radiation pattern of the fundamental mode of the L3-defect structure with $r = 0.30a$ and $d = 0.65a$ is also shown in Fig. 5.3(b) for comparison. As can be observed, the radiation pattern of the dipole mode of the H1-defect structure has a nearly Gaussian profile, whereas such a profile does not occur in the L3-defect structure. The dipole mode can achieve such a simple radiation pattern due to many reasons. First of them is that because the dipole mode has a predominant component of the near-field locating at the center region as shown in Fig. 5.4(a), the Fourier transform of this kind of pattern, which indicates its far-field radiation pattern, will also have a major part at

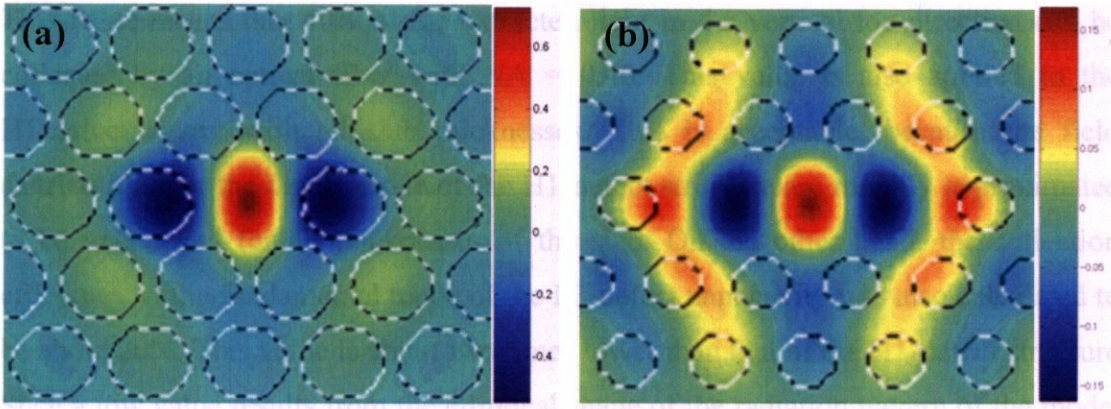


Figure 5.4 Near-field patterns of E_y component of (a) the dipole mode of the H1-defect structure, and (b) the fundamental mode of the L3-defect structure detected at the distance $d/4$ above the surface of the slab.

the center. On the other hand, other modes, for example, quadrupole, monopole, or hexapole mode of the H1-defect cavity, do not have the antinode of near-field at the center, therefore, their radiation patterns contain many components deviated from the center and consequently become complicated. However, with only this explanation, it is still unclear to understand the origin of the Gaussian-like radiation pattern in the dipole mode because the fundamental mode of the L3-defect structure also has such an antinode of near-field at the center as shown in Fig. 5.4(b), still it does not obtain the Gaussian-like radiation like the dipole mode. This can be explained by the shape of the L3-defect cavity. Because the L3-defect cavity has an asymmetric shape, in which the cavity is formed by removing three air holes in the $\Gamma - K$ direction, the confined mode is then stretched along the longitudinal direction of the cavity as shown in the field distribution in Fig. 4.9. Since the near-field is strongly related to the field profile inside the cavity, it also has such a longitudinal distribution. Taking the Fourier transform of this kind of pattern results in the elliptical-shape pattern stretched in the direction perpendicular to the original one as shown in Fig. 5.3(b). On the other hand, in the case of the H1-defect structure, such an asymmetric radiation pattern does not occur due to a symmetric shape of the cavity. Therefore, the radiation pattern of the dipole mode of the H1-defect structure is symmetric and shows the Gaussian-like distribution.

The collection efficiency of the dipole mode of the H1-defect nanocavity was calculated. The numerical aperture of the collection optic was set to be equal to 0.40. For the structure with $r = 0.40a$ and $d = 1.35a$, the collection efficiency is about 40%.

This value means that 40% of the extracted light in the vertical top direction can be collected by an optical fiber with $NA = 0.40$. This value is also applied to the H1-defect cavity with all slab thicknesses. This is acceptable, because the field distributions for the dipole mode of the H1-defect structure are roughly approximated to be unchanged for all thicknesses of the slab. On the other hand, the collection efficiency of the fundamental mode of the L3-defect nanocavity was also calculated to be about 20%. This value is about two times lower than that of the H1-defect structure. Such a low value results from the elliptical shape of the radiation pattern of the mode, not the Gaussian-like radiation pattern as in the case of the dipole mode of the H1-defect structure.

5.4 Total Efficiency of Dipole Mode of H1-Defect Nanocavity

After calculating all three factors of efficiency, the coupling efficiency, the extraction efficiency, and the collection efficiency, in this section the total efficiency

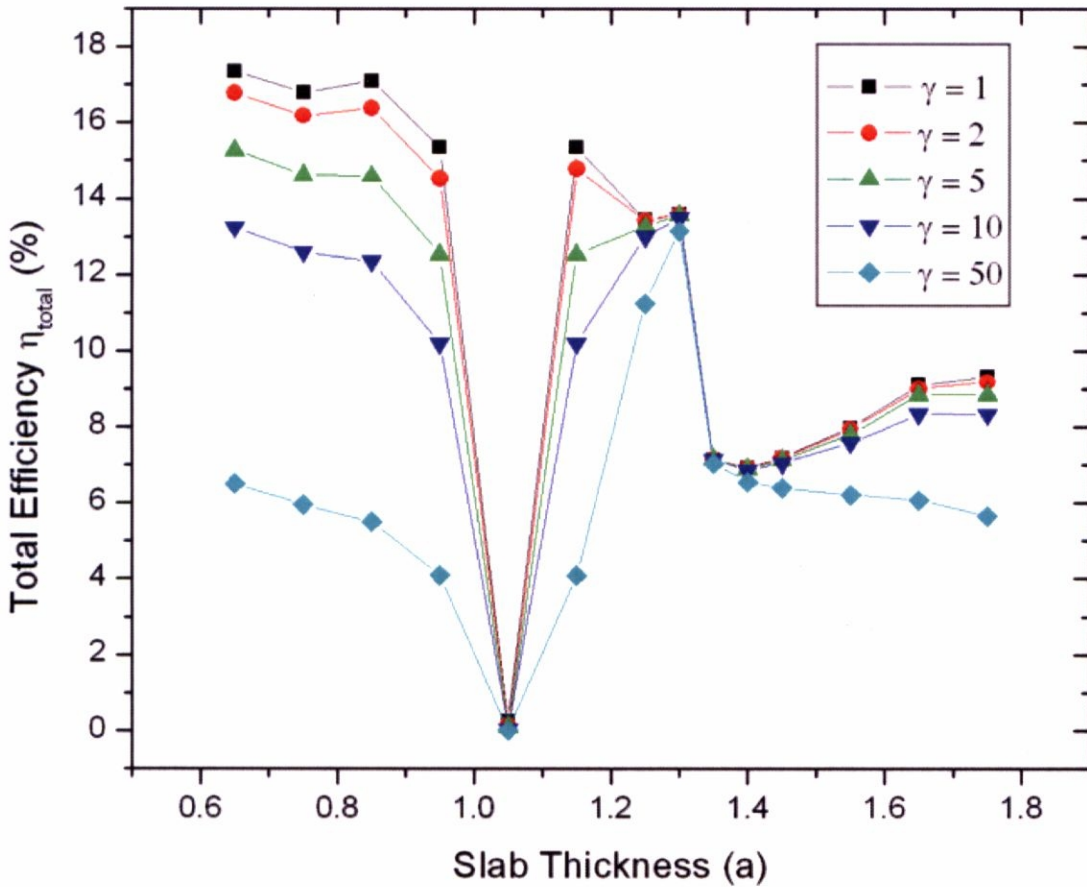


Figure 5.5 Dependence of total efficiency on the slab thickness and nonradiative recombination γ_{nr} for the dipole mode of the H1-defect nanocavity with $r = 0.40a$.

of the dipole mode of the H1-defect nanocavity is evaluated. Figure 5.5 shows the dependence of the total efficiency on the slab thickness for the dipole mode of the H1-defect structure. In this plot, γ_{nr} is varied to various values, $0, 1\gamma_0, 5\gamma_0, 10\gamma_0,$ and $50\gamma_0,$ where was set to be equal to 1GHz corresponding to a radiative lifetime of 1ns. κ_e was set to be 0. The collection efficiency is equal to 40% as calculated in last section. In the thin slab region, the total efficiency is high due to its high extraction efficiency. However, the total efficiency in this region is very sensitive to the nonradiative recombination rate, which is in actual device usually equal to 10 times spontaneous emission rate in free space or around 10 GHz. On the other hand, in the thick slab region, the high total efficiency with insensitivity to the nonradiative recombination occurs at the slab thickness equal to $1.30a.$ The total efficiency is up to 14% at all values of $\gamma_{nr}.$ Furthermore, the dipole mode of the designed cavity with the total Q -factor in the order of 10^4 is supposed to be the optimum structure in order to achieve highest efficiency. Figure 5.6 shows the collection efficiency and the

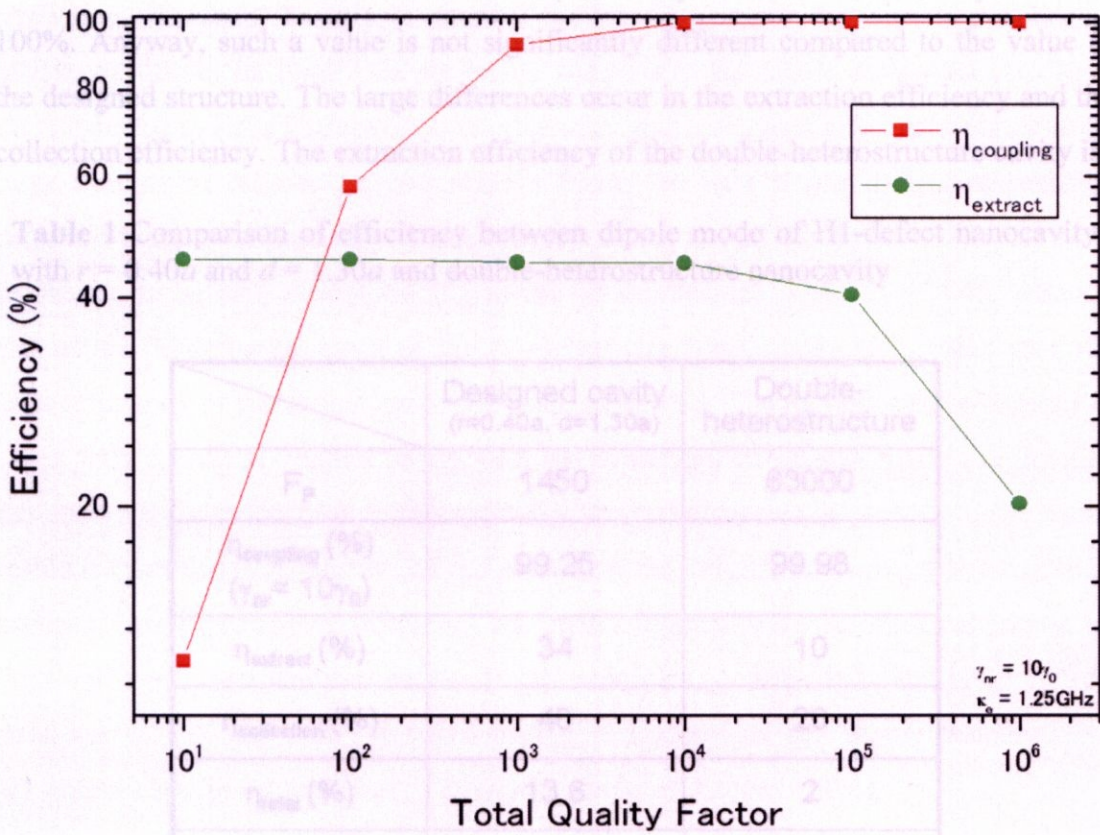


Figure 5.6 Dependence of coupling efficiency and extraction efficiency on total Q-factor. γ_{nr} and κ_e are set to be equal to $10\gamma_0$ and 1.25GHz, respectively.

extraction efficiency as a function of the total Q -factor. The coupling efficiency increases as the total Q -factor increases due to the enhancement of the Purcell factor. On the other hand, the extraction efficiency reduces as the total Q -factor increases due to the cavity decay rate κ_e originated from the imperfection in fabrication process. Usually, κ_e is in the order of 1GHz, which is corresponding to the Q -factor of about 10^6 . As a result, the cavity decay rate κ_e strongly degrades the extraction efficiency of the structure with Q -factor more than 10^4 . From these two tendencies of the efficiency, it can be concluded that the optimum Q -factor for high efficiency is in the order of 10^4 .

In addition, the total efficiency of the designed structure is compared with that of the highest Q -factor nanocavity ever reported so far, the double-heterostructure nanocavity [10]. The results are shown in Table 1. The double-heterostructure nanocavity has the total Q -factor of about 10^6 and mode volume of about $1.2(\lambda/n)^3$. These values allow the cavity to obtain the Purcell factor as high as 63,000. As a result, this structure achieves the extraction efficiency of about 99.98%, very closed to 100%. Anyway, such a value is not significantly different compared to the value of the designed structure. The large differences occur in the extraction efficiency and the collection efficiency. The extraction efficiency of the double-heterostructure cavity is

Table 1 Comparison of efficiency between dipole mode of H1-defect nanocavity with $r = 0.40a$ and $d = 1.30a$ and double-heterostructure nanocavity

	Designed cavity ($r=0.40a$, $d=1.30a$)	Double-heterostructure
F_P	1450	63000
η_{coupling} (%) ($\gamma_{\text{nr}} = 10\gamma_0$)	99.25	99.98
η_{extract} (%)	34	10
$\eta_{\text{collection}}$ (%)	40	20
η_{total} (%)	13.6	2
Nonradiative recombination	Insensitive	Insensitive
Imperfection from fabrication	Insensitive	Sensitive

only about 10% because its Q -factor is in the order of 10^6 . The collection efficiency of the double-heterostructure nanocavity is 20% resulted from its field distribution very closed to those of the fundamental mode of the L3-defect cavity. From these results, the total efficiency of the designed structure has the total efficiency of about 7 times higher than that of the double-heterostructure nanocavity. The efficiencies of both structures are insensitive to nonradiative recombination. However, the double-heterostructure nanocavity is very sensitive to the imperfection of lattice crystal originated during the fabrication process.

5.5 Summary

In this chapter, the dipole mode of the H1-defect cavity with optimized slab thickness has been shown to be a very promising structure for realizing highly-efficient surface emitting light sources due to its ability to achieve optimum efficiency. Firstly, the definition of the total efficiency has been described to be composed of three factors, the coupling efficiency, extraction efficiency, and collection efficiency. The dipole mode of the H1-defect cavity has very high coupling efficiency due to its large Purcell factor. Moreover, the dipole mode has also been demonstrated to have high extraction efficiency and collection efficiency owing to its large number of momentum components inside the light line and its Gaussian-like radiation pattern, respectively. The collection efficiency of the dipole mode has been calculated to be 40% corresponding to the collection lens with $NA = 0.40$, whereas that of the fundamental mode of the L3-defect structure is only 20%. After that, the total efficiency of the dipole mode has been evaluated. The highest total efficiency is about 14% for the H1-defect cavity with $r = 0.40a$ and $d = 1.30a$. Such a high value has shown to be insensitive to the nonradiative recombination as well as to the losses resulted from the imperfection of the lattice crystal originated during the fabrication process. This value of total efficiency has been compared with the value calculated for the double-heterostructure nanocavity, in which its Q -factor is in the order of 10^6 . And the results show the 7 times higher efficiency of the dipole mode of the H1-defect nanocavity than that of the double-heterostructure nanocavity.

Chapter 6

Conclusions

6.1 Summary of This Thesis

In this thesis, the design of the photonic crystal nanocavity for the realization of highly-efficient surface-emitting light sources, such as low-threshold nanolasers, and single photon emitters, has been investigated. In order to achieve that goal, the air-bridge slab H1-defect nanocavity with optimized slab thickness has been shown to be a very promising structure, because its dipole mode can achieve very large Purcell factor, high extraction efficiency, and simple radiation pattern, which yields to the high total efficiency. The design of H1-defect nanocavity in this research is totally new and original.

Firstly, in chapter 2, the basis for the principle of photonic crystal has been reviewed. Maxwell's equations have been described as an important tool to study the behavior of electromagnetic waves in photonic crystal. And then, in chapter 3, the three-dimensional finite-difference time-domain (FDTD) method, which is the direct solution method for Maxwell's time dependent curl equations, has been explained. The 3D FDTD method has been adopted as a computational method to investigate the characteristics of cavity, such as, resonant frequency, field distribution, Q -factor, Purcell factor and mode volume.

In this research, the photonic crystal slab structure has been exploited in the design owing to its simplicity in practical fabrication and its ability to strongly confine light within a cavity in three dimensions, which are a combination of total internal reflection and Bragg reflection. However, this kind of structure has been suffered from a long-standing problem due to the radiation loss in vertical direction, which is corresponding to a large number of momentum components lying within the light cone. To achieve a cavity very high Q -factor in all directions, the design of the H1-defect cavity has been presented and discussed in chapter 4. By just changing the slab thickness, the very high Q -factor, in which the maximum value is about 16,200, has been achieved in the structure, in which the slab is so thick that the photonic band gap is closed. The structure parameters of the highest Q structure are $r = 0.40a$ and $d = 1.35a$. In the structures with different values of radius of air holes, such a peak has

also been obtained, but with less sharpness and lower value of Q -factor. From the relation between the cavity size in in-plane direction and the slab thickness, which determines the cavity size in vertical direction, as well as the observation of the splitting fields coming closer when the slab thickness increases; it may be assumed that the confinement mechanism, which makes such a kind of high Q cavity, is originated from a symmetric cubic shape of the cavity. This assumption is considered reasonable because both $Q_{//}$ and Q_{\perp} change together after the gap is closed, which means that the additional confinement mechanism affects all three dimensions of the cavity. Moreover, such a special confinement mechanism could not be observed in any thicker slab regions than the studied region. To confirm this assumption, the same study of the dependence of Q -factor on the slab thickness has been applied to the L3-defect structure for comparison. The L3-defect structure is suitable for this aim due to its asymmetric cavity shape. No peak of Q -factor in the region, where the gap is closed, has been observed in this structure. As a result, it can be confirmed that the symmetric cubic shape of the cavity is really the cause of the very high Q -factor of the dipole mode even when the photonic band gap is already closed. The large Purcell factor of about 2,870 has been achieved, and the mode volume is in the order of half wavelength.

In chapter 5, the dipole mode of the H1-defect cavity with optimized slab thickness has also been shown to be a very promising structure for realizing highly-efficient surface emitting light sources due to its ability to achieve optimum efficiency, corresponding to high coupling efficiency, extraction efficiency, and collection efficiency in the same structure. The dipole mode of the H1-defect cavity has very high coupling efficiency due to its large Purcell factor. Moreover, the dipole mode has also been demonstrated to have high extraction efficiency and collection efficiency owing to its large number of momentum components inside the light line and its Gaussian-like radiation pattern, respectively. The collection efficiency of the dipole mode has been calculated to be 40% corresponding to the collection lens with $NA = 0.40$, whereas that of the fundamental mode of the L3-defect structure is only 20%. The highest total efficiency is about 14% for the H1-defect cavity with $r = 0.40a$ and $d = 1.30a$. Such a high value has shown to be insensitive to the nonradiative recombination as well as to the losses resulted from the imperfection of the lattice crystal originated during the fabrication process. This value of total efficiency has been compared with the value calculated for the double-heterostructure nanocavity,

in which its Q -factor is in the order of 10^6 , the highest Q cavity reported so far. And the results show the 7 times higher efficiency of the dipole mode of the H1-defect nanocavity than that of the double-heterostructure nanocavity.

From all of these results, it can be concluded that, with the design H1-defect nanocavity presented in this research, the highly-efficient surface-emitting light sources, such as, low-threshold nanolasers, and single photon emitters, with optimum efficiency can be realized.

6.2 Future Prospects

From the results presented in this research, the following items will be discussed in the future:

1. Further Increase of Extraction Efficiency

In order to obtain higher efficiency than the results shown in this thesis, the ratio of vertical Q -factor to in-plane Q -factor has to be increased. One possible way is to increase the number of periods of air holes. The other approach to improve extraction efficiency is to apply the design cavity to an asymmetric structure, which has some kinds of reflectors at the bottom of the slab. As already mentioned, the extraction efficiency in the air bridge structure is limited to only 50% due to its symmetry in vertical direction. Therefore, if a reflector can be added to the bottom-side of the slab, most light output will be radiated out from top-side of the slab surface and the limitation of 50% will be overcome. One possible structure for this approach is a Quasi-3D structure [35], which is a combination of a two-dimensional photonic crystal and a one-dimensional distributed Bragg reflector.

2. Fabrication of Practical Devices

The design cavity will be practically fabricated. By introducing quantum dots to the design nanocavity as an active material, the high Q -factor of the cavity will increase a coupling strength between the quantum dots and the cavity mode. This results in enhancement of spontaneous emission rate, spontaneous emission coupling factor, and decrease of decay time of the quantum dots. With these results as well as the high extraction efficiency of the design cavity and its simple radiation pattern, the

low-threshold nanolasers and the high efficiency, high repetition rate single photon emitters are possible to be realized.

References

- [1] E. M. Purcell: Phys. Rev. **69** (1946) 681.
- [2] E. Yablonovitch: Phys. Rev. Lett. **58** (1987) 2059.
- [3] O. Painter, R. K. Lee, A. Scherer, A. Yariv, J. D. O'Brien, P. D. Dapkus and I. Kim: Science **284** (1999) 1819.
- [4] H. Y. Ryu, H. G. Park and Y. H. Lee: IEEE J. Sel. Top. Quantum Electron. **8** (2002) 891.
- [5] C. Santori, D. Fattal, J. Vučković, G. S. Solomon and Y. Yamamoto: Nature **419** (2002) 594.
- [6] J. Vučković, D. Fattal, C. Santory, G. S. Solomon and Y. Yamamoto: Appl. Phys. Lett. **82** (2003) 3596.
- [7] J. Vučković, M. Lončar, H. Mabuchi and A. Scherer: IEEE J. Quantum Electron. **38** (2002) 850.
- [8] Y. Akahane, T. Asano, B. S. Song and S. Noda: Nature **425** (2003) 944.
- [9] Y. Akahane, T. Asano, B. S. Song and S. Noda: Opt. Express **13** (2005) 1202.
- [10] B. S. Song, S. Noda, T. Asano and Y. Akahane: Nature Mat. **4** (2005) 207.
- [11] K. Srinivasan, P. E. Barclay and O. Painter: Opt. Express **12** (2004) 1458.
- [12] J. Vučković and Y. Yamamoto: Appl. Phys. Lett. **82** (2003) 2374.
- [13] H. G. Park, J. K. Hwang, J. Huh, H. Y. Ryu, S. H. Kim, J. S. Kim and Y. H. Lee: IEEE J. Quantum Electron. **38** (2002) 1353.
- [14] M. Pelton, J. Vučković, G. S. Solomon, A. Scherer and Y. Yamamoto: IEEE J. Quantum Electron. **38** (2002) 170
- [15] M. Pelton, C. Santori, J. Vučković, B. Zhang, G. S. Solomon, J. Plant, and Y. Yamamoto: Phys. Rev. Lett. **89** (2002) 233602.
- [16] J. C. Maxwell: Phil. Trans. **155** (1865) 459.
- [17] N. W. Ashcroft and N. D. Mermin: Solid State Physics (Holt Saunders, Philadelphia, 1976).
- [18] L. C. Andreani and M. Agio: IEEE J. Quantum Electron. **38** (2002) 891.
- [19] S. G. Johnson, S. Fan, P. R. Villeneuve and J. D. Joannopoulos: Phys. Rev. B **60** (1999) 5751.
- [20] M. Kafesaki, C. M. Soukoulis and M. Agio: J. Appl. Phys. **96** (2004) 4033.
- [21] K. S. Yee: IEEE Trans. Antennas Propagat. **AP-14** (1966) 302.

- [22]A. Taflove: Computational Electrodynamics: The Finite-Difference Time-Domain Method (Artech House, Norwood, MA, 2000) 2nd ed.
- [23]J. P. Berenger: J. Comput. Phys. **114** (1994) 185.
- [24]J. D. Jackson: Classical Electrodynamics (Wiley, New York, 1962).
- [25]O. Painter, J. Vučković and A. Sherer: J. Opt. Soc. Am. B **16** (1999) 275.
- [26]T. Yoshie, J. Vučković, A. Sherer, H. Chen and D. Deppe: Appl. Phys. Lett. **79** (2001) 4289.
- [27]Z. Zhang and M. Qiu: Opt. Lett. **30** (2005) 1713.
- [28]P. R. Villeneuve, S. Fan, S. G. Johnson and J. D. Joannopoulos: IEE Proc.: Optoelectron **145** (1998) 384.
- [29]H. Y. Ryu, M. Notomi and Y. H. Lee: Appl. Phys. Lett. **83** (2003) 4294.
- [30]J. M. Gérard, B. Sermage, B. Gayral, R. Legrand, E. Costard and V. Thierry-Mieg: Phys. Rev. Lett. **81** (1998) 1110.
- [31]I. K. Hwang, S. K. Kim, J. K. Yang, S. H. Kim, S. H. Lee and Y. H. Lee: Appl. Phys. Lett. **87** (2005) 131107.
- [32]I. K. Hwang, G. H. Kim and Y. H. Lee: J. Korean Phys. Soc. **47** (2005) 434.
- [33]D. Englund, D. Fattal, E. Waks, G. Solomon, B. Zhang, T. Nakaoka, Y. Arakawa, Y. Yamamoto and J. Vučković: Phys. Rev. Lett. **95** (2005) 013904.
- [34]H. Altug and J. Vučković: Opt. Express **13** (2005) 8819.
- [35]M. Ito, S. Iwamoto and Y. Arakawa: Jpn. J. Appl. Phys. **43** (2004) 1990.

List of Publications

Journal Papers

- [1] A. Tandaechanurat, S. Iwamoto and Y. Arakawa: “Design of Large Purcell Factor and High Efficiency Photonic Crystal H1-defect Nanocavities by Optimizing Slab Thickness”, (to be submitted).

Conference Papers

- [1] A. Tandaechanurat, S. Iwamoto and Y. Arakawa: “High Quality factor Photonic Crystal H1-defect Nanocavities with Optimized Slab Thickness”, (53th Spring Meet, 2006); Japan Society of Applied Physics and Related Societies, 24p-L-5.

Acknowledgement

I would like to express my deep and sincere gratitude to my supervisor, Professor Arakawa Yasuhiko for giving me a great opportunity to join this laboratory. His guidance, constructive comments, and important support have provided a good basis for the present thesis.

I am deeply grateful to my supervisor, Dr. Iwamoto Satoshi, for all of his supports including an important guidance during my first step into FDTD coding studies. His extensive discussions around my work and his valuable advice made me able to fulfill this thesis. His wide knowledge and his logical way of thinking have been of great value for me.

I wish to express my warm and sincere thanks to Mr. Nishioka Masao, Mr. Ishida Satomi, and Dr. Nomura Masahiro for lending me their accounts of using supercomputer.

I would like to thank Dr. Kitamura Masatoshi, Mr. Arita Munetaka, and all other members of Arakawa laboratory for their advices and supports.

My special gratitude is due to my family. Without their encouragement and understanding it would have been impossible for me to finish this work.

I owe my loving thanks to Ms. Pim Srithammawoot for her loving support and encouragement.

The financial support of the IT program, MEXT, is gratefully acknowledged.